Shehata *et al.*
Journal of Engineering and Applied Science (2023) 70:63
https://doi.org/10.1186/s44147-023-00237-1

Journal of Engineering and Applied Science

RESEARCH Open Access

A suggested dynamic soil – structure interaction analysis

Osama E. Shehata[1], Ahmed Fady Farid[1*] and Youssef F. Rashed[1]

*Correspondence:
ahmedfadyfarid@eng1.cu.edu.eg

[1] Department of Structural Engineering, Cairo University, Giza, Egypt

Abstract

In this paper, a new methodology for time domain analysis of buildings on raft foundations considering soil – structure interaction is proposed. Sub-structuring technique is used to separate the building as super-structure and the underneath soil as sub-structure. The super-structure can be modeled using any numerical method. However, in this paper the super-structure is modeled via the BEM to consider the real interaction area between column and slabs. The dynamic load is considered as an earthquake acceleration record that can be transformed to equivalent dynamic loads acting on the super-structure floors. The sub-structure is analyzed using the dual reciprocity boundary element method as closed domain. New iterative coupling technique is proposed between the super and sub-structures to reduce the computational effort and required storage. An example is presented to demonstrate the strength and the practicality of the proposed methodology.

Keywords: Dynamic analysis, , Soil – structure interaction, Iterative solution, Sub-structuring, Dual reciprocity method

Introduction

Dynamic analysis of structures including soil-structure interactions (SSI) affects the structural design process. In recent research [1], dynamic analysis including SSI is effective in performance-based design. In addition, control of buildings with dampers is affected by considering SSI [2]. Time domain analysis is more reasonable for transient response of structures as the response variance with time can be directly obtained [3]. The time domain analysis of buildings including SSI can be carried out using sub-structuring technique. The super-structure and the sub-structure are analyzed separately and then coupling analysis between the super and sub-structure is considered.

The super-structure can be modeled using FEM, most common numerical method, or using BEM. FEM model of the super-structure requires domain discretization for floors. In addition, vertical elements can be modeled as 1D frame element as presented in [4–6], for simplicity, or using 3D solid elements as presented in [7]. Modeling the columns using 3D solid elements ensure better area contact modeling compared to frame element but it is more complicated model in practical problems. On the other hand, BEM can be used to model the super-structure to ensure area contact modeling between vertical

elements and slabs in addition no domain discretization is required [8, 9]. The effect of the super-structure vertical elements model is discussed in Sect. 5. In this paper, the wave excitation at foundation level is transformed to equivalent elastodynamic loading as presented in [10].

The soil model, in the building analysis including SSI, can be presented using simplified [11], FEM [12–15], continuous [16, 17], half space [18–22], dual reciprocity method (DRM) [23–30], and time differencing models [31, 32]. The elastic soil media can be modeled with simplified physical model, equivalent spring-dashpot system, as presented in [11]. The soil elastic media model using FEM presents the fact of semi-infinite domain. Where the soil volume should be extended to sufficient distance from the loading area [4–6] or applying equivalent infinite elements on the boundaries [12–15].

The soil is extended to sufficient distance after the building foundation in the dynamic analysis of two adjacent buildings presented in [5] and the case study building in Lisbon is presented in [6]. Perfect matched layer and domain reduction methods can be employed on the boundary to reduce the extended soil volume as presented in [4].

Concerning the semi-infinite domain in FEM, Lysmer and Kuhlemeyer [12] firstly discussed using the viscous boundary to represent infinite modeling of soil. Smith and Warwick [13] proposed non-reflecting boundaries to avoid wave reflection that affects the boundary conditions (traction and displacement). Bakhtaou et al.[14] presented 2D analysis of elastic block on soil using infinite elements coupled with absorbing layer. While Su and Wang [15] proposed an equivalent dynamic infinite element that consider the advantages of elastodynamic infinite element presented in [12] and viscous boundaries in [13]. The implementation of infinite element and extending the soil volume are not practical ways due to the required large computational efforts.

BEM can be employed in elastic soil media modeling using different methods [33]. The continuous model that tends to calculate the dynamic stiffness of foundation by semi-analytical solution of the differential equation as presented in [16]. A simple problem of disc on elastic half space is presented in [16] with relaxed boundary conditions where as a strip foundation is analyzed with full bond of the soil is presented in [17]. The continuous model can be presented only for simple cases of loading and boundary conditions [33].

The soil can be modeled as elastic half space in the analysis of foundations as presented in [18–22]. The proposed formulation in [18–22] employs Stoke's solution that is time dependent solution, in which, the kernels and matrices are calculated at each time step which is not suitable for practical applications.

Alternatively, the soil can be modeled using DRM as 3D closed domain by employing the static fundamental solutions instead of time dependent fundamental solution. The implementation of static fundamental solution in dynamic analysis leads to domain integral for the body inertia terms. Solving the domain integral requires domain discretization [34] or transforming the domain integral to the boundary using DRM [23–30]. DRM is presented in 2D dynamic analysis as presented in [23–26]. Partidge et al.[27] presented employing the DRM in 3D elastodynamic problem. Beskos et al.[28] applied the DRM in free and forced vibration of 3D elastic solids. Kog and Gaul [29] employed the DRM in the time domain analysis of anistropic solids instead of using the complex dynamic fundamental solution. Galvis et al.[30] presented an open-source 3D BEM software using DRM for the dynamic

analysis of solids. The implementation of DRM in [27–30] is to approximate the domain integral instead of domain discretization for closed domain problems. Therefore, for practical time domain analysis, the DRM can be applied to model the soil as closed domain without domain discretization.

The coupling of the super and sub-structures can be directly as presented in [4–6] or using iterative method [35, 36]. Direct coupling of the super and sub-structures leads to large memory required and consumes larger computational effort [4–6]. Alternatively, iterative coupling permits the analysis of the two structures separately with different software packages. In addition, iterative coupling reduces the required storage compared to that of the direct coupling. Iterative coupling is presented in dynamic analysis in the work of Lei et al.[35] between FEM and BEM in 2D analysis. Iterative coupling is presented in [36] to couple the super-structure and elastic half space under static loading.

In this paper, a new proposed methodology for time domain analysis of 3D buildings including SSI is presented. The earthquake acceleration excitation is transformed to equivalent dynamic loads acting on the super-structure as presented in [10]. The super-structure can be modeled using any numerical method. In this paper, the super-structure is modeled using BEM to represent the real area model between vertical elements and slabs. The sub-structure is analyzed using boundary element formulation based on the static fundamental solution. The dual reciprocity method is employed to transform the domain integral to the boundary. New proposed iterative coupling scheme is presented between the super and sub-structures. Numerical example is presented to demonstrate the practicality of the proposed methodology. The effect of varying the number of coupling area cells is discussed.

Methods

Time domain analysis of super-structure

In this section, the time domain analysis of the super-structure is presented. The super-structure is modeled as slabs supported on vertical elements. The vertical elements are supported on raft foundation. The building can be modeled using any numerical method to compute its relevant stiffness and mass matrices. Each floor is modeled as a diaphragm with three degrees of freedom (DOF), two translations and one rotation. The building stiffness and mass matrices are condensed at the diaphragm DOFs in addition to the vertical coupling DOFs at raft – soil interface as shown in Fig. 1. In the proposed model, the raft foundation is a part of the super-structure. The raft is modeled using BEM and its stiffness matrix is calculated condensed at coupling DOFs following the proposed formulation in [37, 38]. The tall building stiffness and mass matrices are calculated as presented in [8]. Therefore, the super-structure stiffness matrix is formed by assembling the tall building and raft foundation stiffness matrices and can be written as follows:

$$\left[K_{super}\right]_{N_1\times N_1} = \begin{bmatrix} \left[K_{super11}\right]_{3N_{FL}\times 3N_{FL}} & \left[K_{super12}\right]_{3N_{FL}\times N_{Cells}} \\ \left[K_{super21}\right]_{N_{Cells}\times 3N_{FL}} & \left[K_{super22}\right]_{N_{Cells}\times N_{Cells}} \end{bmatrix} \tag{1}$$

$$\left[M_{super}\right]_{N_1\times N_1} = \begin{bmatrix} \left[M_{super11}\right]_{3N_{FL}\times 3N_{FL}} & [0]_{3N_{FL}\times N_{Cells}} \\ [0]_{N_{Cells}\times 3N_{FL}} & \left[M_{super22}\right]_{N_{Cells}\times N_{Cells}} \end{bmatrix} \tag{2}$$

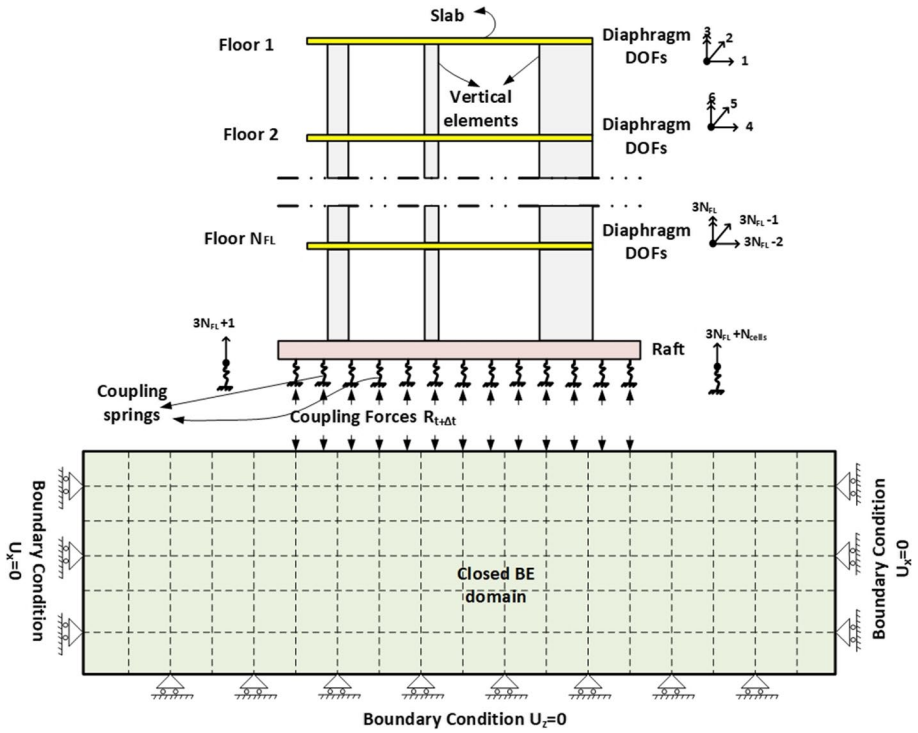

Fig. 1 Proposed sub-structuring analysis

It has to be noted that, at the raft – soil interface, the sub-matrix $\left[K_{super22}\right]_{N_{Cells}\times N_{Cells}}$ is the assembly of two matrices:

$$\left[K_{super22}\right]^{t+\Delta t}_{N_{Cells}\times N_{Cells}} = \left[K^{fixed}_{super22}\right]_{N_{Cells}\times N_{Cells}} + \left[K_{springs}\right]^{t+\Delta t}_{N_{Cells}\times N_{Cells}} \tag{3}$$

where $\left[K_{springs}\right]^{t+\Delta t}$ is set to be zeros only in the first time step. Whereas, in the following time steps, $\left[K_{springs}\right]^{t+\Delta t}$ is calculated based on the sub-structure displacement using the proposed iterative coupling technique as presented in Sect. 4.

The dynamic loading is considered as acceleration time history records. In the proposed analysis, the acceleration time history is transformed to equivalent dynamic loads on the super-structure $P^{t+\Delta t}$. The equivalent dynamic loads are calculated as the product of mass matrix and ground acceleration record [10]. Concerning the numerical accuracy, the vertical elements modeling has a strong effect on the lateral response of the building [39]. The vertical elements using BEM can be modeled as one area cell. Increasing the number of area cells gives a better response. A numerical verification of this point is presented in Sect. 5.

Time stepping DRM analysis of sub-structure

In this paper, the sub-structure (soil) is modeled using 3D BEM formulation based on static fundamental solution. The Dual Reciprocity Method (DRM) is employed to transform the domain integral to the boundary. The dynamic loading on the sub-structure is the reactions (coupling forces) from the super-structure $R_{t+\Delta t}$(recall Fig. 1) where

(t + Δt) is a certain time step. In this paper, the sub-structure is modeled as an extended closed domain to avoid the wave reflections at boundaries.

The solution of the differential equation presented in Eq. (4) can be separated into particular solution and complementary solution. After substituting the particular solution with an approximating function [25], the boundary integral equation can be written in a matrix form as presented in Eq. (5).

$$\mu u_{i,jj} + (\lambda + \mu) u_{j,ji} = \rho \ddot{u}_i \tag{4}$$

$$\begin{aligned} &\left[H_{sub}\right]_{3M\times 3M}\left\{u_{sub}\right\}_{3M\times 1} - \left[G_{sub}\right]_{3M\times 3M}\left\{t_{sub}\right\}_{3M\times 1} \\ &= -\rho\left(\left[H_{sub}\right]_{3M\times 3M}\left[\widehat{u}\right]_{3M\times 3K} - \left[G_{sub}\right]_{3M\times 3M}\left[\widehat{t}\right]_{3M\times 3K}\right)[F]^{-1}_{3K\times 3M}\left\{\ddot{u}_{sub}\right\}_{3M\times 1} \end{aligned} \tag{5}$$

Simplifying Eq. (5), the equation can be written in a form of FEM as follows:

$$[M_{sub}]_{3M\times 3M}\{\ddot{u}_{sub}\}_{3M\times 1} + [H_{sub}]_{3M\times 3M}\{u_{sub}\}_{3M\times 1} = [G_{sub}]_{3M\times 3M}\{t_{sub}\}_{3M\times 1} \tag{6}$$

where $[M_{sub}]$ is a new equivalent mass matrix calculated using the DRM formulation as follows:

$$[M_{sub}]_{3M\times 3M} = -\rho\left([H_{sub}]_{3M\times 3M}[\widehat{u}]_{3M\times 3K} - [G_{sub}]_{3M\times 3M}\left[\widehat{t}\right]_{3M\times 3K}\right)[F]^{-1}_{3K\times 3M} \tag{7}$$

By implementing a suitable finite difference scheme, Houbolt finite difference scheme [39], Eq. (6) at time step (t + Δt) can be written as follows:

$$\begin{aligned} \left[\frac{2}{\Delta t^2}[\mathrm{M_{sub}}]_{3M\times 3M} + [H_{sub}]_{3M\times 3M}\right]\{u^{t+\Delta t}_{sub}\}_{3M\times 1} &= [\mathrm{G}_{sub}]_{3M\times 3M}\{t^{t+\Delta t}_{sub}\}_{3M\times 1} \\ &+ \frac{[M_{\mathrm{sub}}]_{3M\times 3M}}{\Delta t^2}[5\{u^{t}_{sub}\}_{3M\times 1} \\ &- 4\{u^{t-\Delta t}_{sub}\}_{3M\times 1} + \{u^{t-2\Delta t}_{sub}\}_{3M\times 1}] \end{aligned} \tag{8}$$

To solve the system of equations in Eq. (8), the matrices $\left[\frac{2}{\Delta t^2}[M_{\mathrm{sub}}] + [H_{\mathrm{sub}}]\right]$,$[M_{\mathrm{sub}}]$, and $[G_{\mathrm{sub}}]$ must be rearranged according to known and unknown fields. The final matrix form of the transient analysis is presented as follows:

$$\begin{aligned} \left[\mathrm{A}_{sub}\right]_{3M\times 3M}\left\{x^{t+\Delta t}_{sub}\right\}_{3M\times 1} &= [G_{1sub}]_{3M\times 3M}\{b^{t+\Delta t}_{sub}\}_{3M\times 1} \\ &+ \frac{\left[M_{\mathrm{sub}}\right]_{3M\times 3M}}{\Delta t^2}[5\{u^{t}_{sub}\}_{3M\times 1} \\ &- 4\{u^{t-\Delta t}_{sub}\}_{3M\times 1} + \{u^{t-2\Delta t}_{sub}\}_{3M\times 1}] \end{aligned} \tag{9}$$

The sub-structure corresponding matrices $[\mathrm{A}_{sub}]$, $[G_{1sub}]$, $[M_{\mathrm{sub}}]$ are calculated to be implemented in the iterative coupling presented in next section.

The proposed iterative coupling

The coupling between super and sub-structures can be performed using direct or iterative techniques. The iterative technique reduces the required storage and computational

efforts as the super and sub-structures can be analyzed separately and permits using different models. In this section, an iterative coupling technique is proposed where the time domain analysis is performed in each iteration on the super and sub-structures. It has to be noted that the super- and sub-structures should be analyzed using the same time step for coupling. The time step of the sub-structure is commonly the dominant time step; therefore, the time step is determined by trials for the sub-structure first then considered in the overall analysis. An initial time step is determined as $\Delta t = \frac{L}{\sqrt{\frac{E}{\rho}}}$ [40] where L is the mesh element length, E is material modulus of elasticity, and ρ is material density. The time domain analysis of super-structure using Houbolt's numerical scheme [39] can be written in matrix form as follows:

$$\begin{aligned}&\left[\frac{2}{\Delta t^2}\left[\mathrm{M}_{\mathrm{super}}\right]_{N_1\times N_1}+\left[K_{\mathrm{super}}\right]_{N_1\times N_1}\right]\left\{u^{t+\Delta t}_{\mathrm{super}}\right\}_{N_1\times 1}\\&=\left\{P^{t+\Delta t}\right\}_{N_1\times 1}+\frac{\left[\mathrm{M}_{\mathrm{super}}\right]_{N_1\times N_1}}{\Delta t^2}\left[5\left\{u^{t}_{\mathrm{super}}\right\}_{N_1\times 1}-4\left\{u^{t-\Delta t}_{\mathrm{super}}\right\}_{N_1\times 1}+\left\{u^{t-2\Delta t}_{\mathrm{super}}\right\}_{N_1\times 1}\right]\end{aligned}\tag{10}$$

The dynamic analysis is carried out on the super-structure at each time step to compute the reactions (coupling forces) $R_{t+\Delta t}$. Hence, the calculated reactions are applied as dynamic loads acting on the sub-structure as presented in Eq. (9). Equivalent coupling spring stiffness, at each coupling area cell, is calculated by dividing the dynamic load (coupling force) by the displacement of this cell at each time step. Hence, the super-structure stiffness matrix $\left[K_{springs}\right]$(recall Eq. (3)) is updated. In other words, the sub-matrix $\left[K_{super22}\right]$ is updated in each time step during each iteration.

The proposed iterative coupling technique is implemented in a computer code. The super-structure stiffness and mass matrices are extracted via any numerical method as presented in Eqs. (1 and 2). The sub-structure required matrices (recall Eq. (9)) are extracted via 3D boundary element method. Figure 2 demonstrates a flow chart of the proposed iterative technique. In the first iteration, the super-structure reactions (coupling forces) are calculated by analyzing the building over fixed base or $\left[K_{springs}{}^{t+\Delta t}\right]$ can be initially assumed. Concerning the convergence in the proposed iterative analysis, the variation of the super-structure lateral displacement values is considered as the convergence condition. The convergence tolerance in the proposed analysis can be considered as user input value and the default value is set to be 5%.

Numerical effects of vertical elements different models

In order to demonstrate the effect of the employed numerical model on the results, a five-story building presented in Fig. 3 is considered on fixed base to study the appropriate super-structure model. The slab thickness is 20 cm, and each floor is supported on 16 square columns having the same dimensions (a × a). The raft foundation thickness is 40 cm. The material properties of the super-structure are considered with Young's modulus 2×10^7 kN/m^2 and Poisson's ratio equals to 0.2. The top lateral displacement is presented to discuss the effect of vertical elements area modeling. The super-structure is analyzed on fixed base under linear increasing acceleration of 0.5 m/sec^2 at 2 Sec.

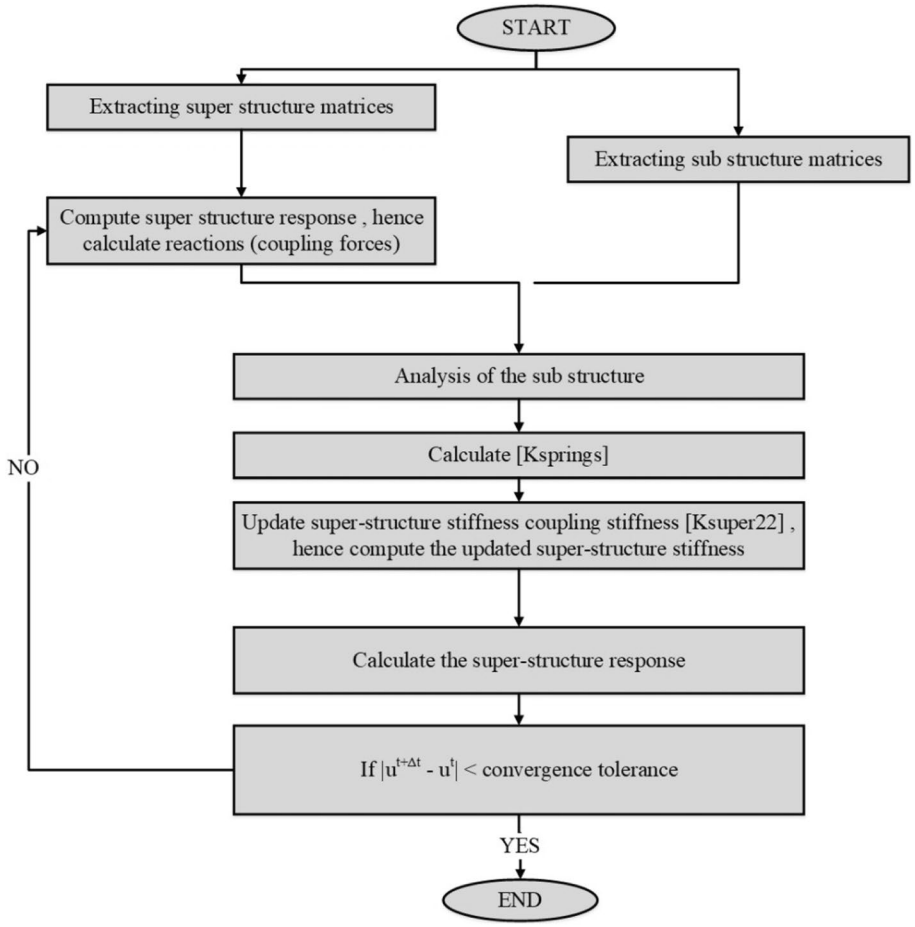

Fig. 2 Flowchart of the proposed iterative coupling technique

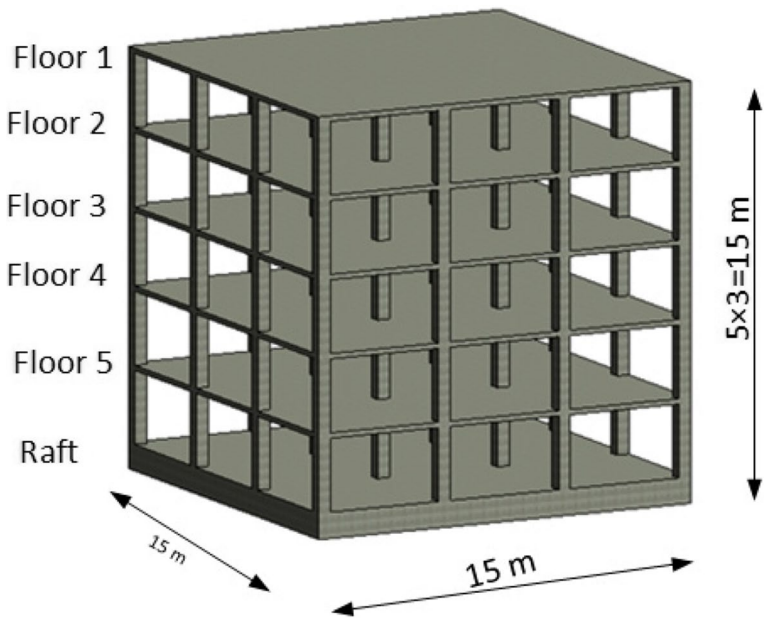

Fig. 3 Three-dimensional model of five stories building on raft foundation

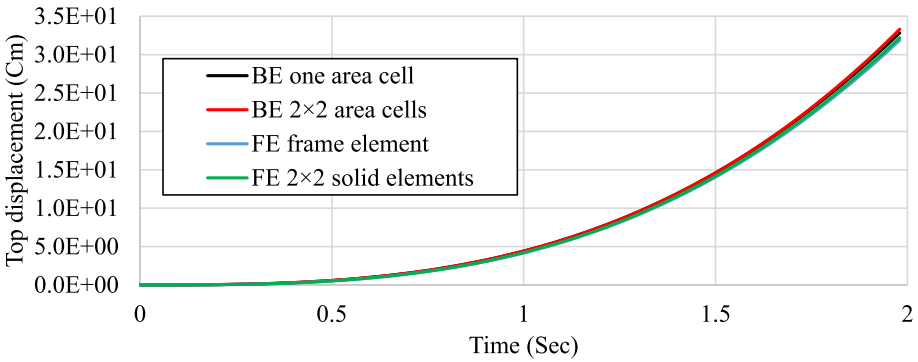

Fig. 4 Top lateral displacement for the case of column dimensions 0.1 × 0.1 m

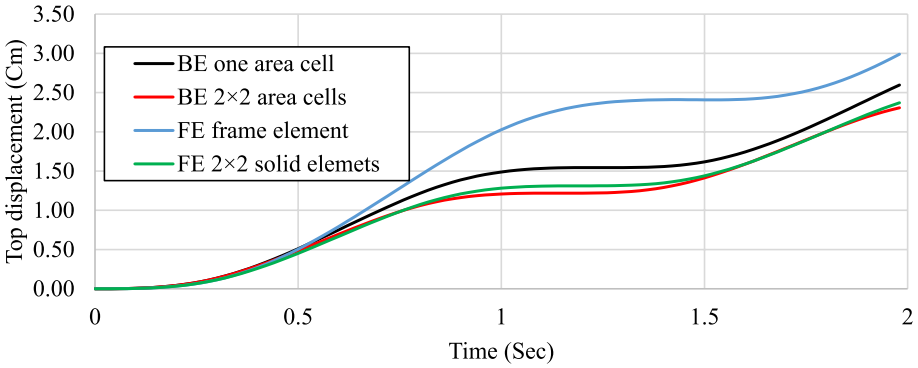

Fig. 5 Top lateral displacement for the case of column dimensions 0.3 × 0.3 m

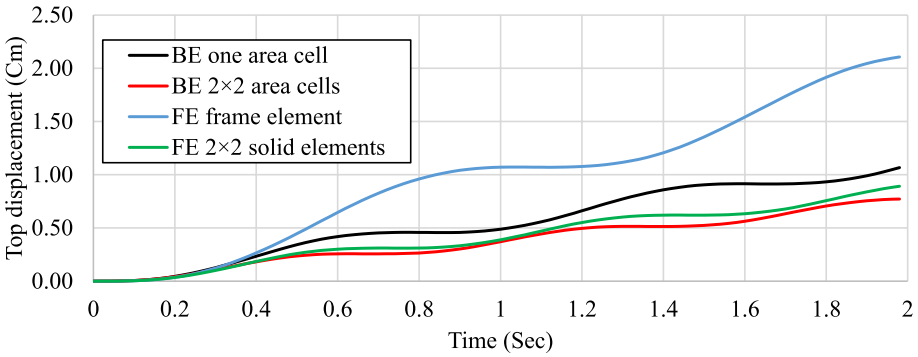

Fig. 6 Top lateral displacement for the case of column dimensions 0.5 × 0.5 m

The dynamic analysis of building on fixed base is carried out with different square column dimensions (a × a); 0.1 × 0.1, 0.3 × 0.3, 0.5 × 0.5 m. Each case is analyzed twice using FEM (frame element, and 2 × 2 solid elements) and twice using BEM (one area cell, and 2 × 2 area cells). The top lateral displacements for three cases 0.1 × 0.1 m, 0.3 × 0.3 m, and 0.5 × 0.5 m are demonstrated in (Figs. 4, 5 and 6).

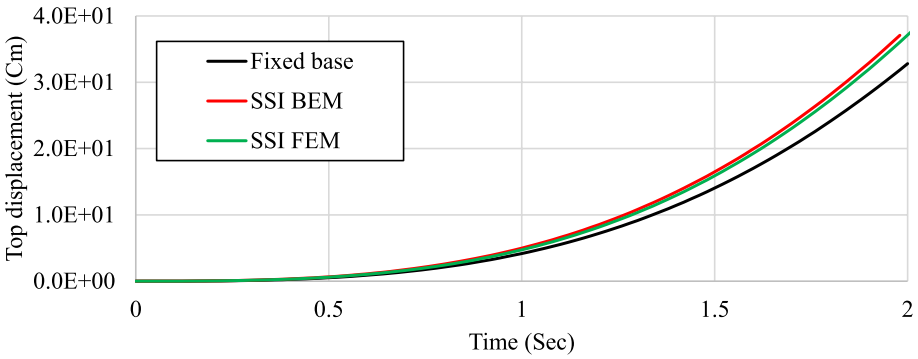

Fig. 7 Top lateral displacement including SSI effect

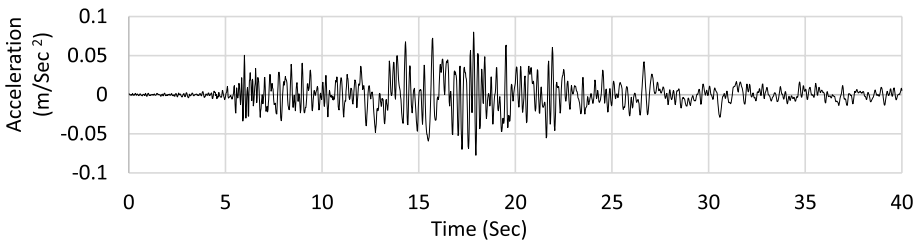

Fig. 8 Earthquake acceleration record considered in example 7.1 case 3

From the presented results, the area modeling of column is critical in the lateral response of the structure. For the case of slender column, BEM and FEM give the same response. On the other hand, increasing the column dimensions increases the difference between FEM and BEM results. FEM model with frame elements gives inaccurate results as the columns dimensions increases. The frame element model error with respect to solid elements model is 26%, 225% for 0.3×0.3, 0.5×0.5 m respectively. The BEM one area cell model error with respect to four area cells is 11%, 38% for 0.3×0.3, 0.5×0.5 m respectively. Therefore, the solid elements modeling of column in FEM is essential to get more realistic response which is more compatible with 2×2 area cells in the proposed BEM analysis.

Results and discussion

In this section, a verification example for the proposed analysis is presented. In addition, a numerical example is presented and compared with results obtained from FE analysis to demonstrate the strength of the proposed technique. The effect of the number of coupling cells is presented.

Verification example

In this section, the same building that previously considered in Sec. 5 is reconsidered here for verification purpose of the proposed model. The case 0.1×0.1 m columns is carried out to minimize the effect of column modeling on the numerical results. The top lateral displacement is presented in Fig. 7. The response from the proposed analysis is in a good agreement with FEM results.

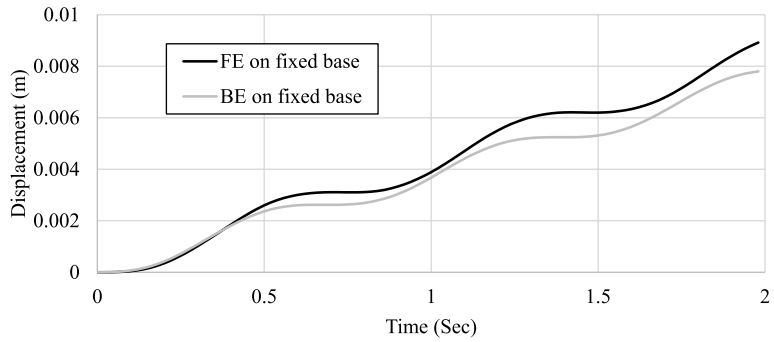

Fig. 9 Top lateral displacement on fixed base under linear load in example 7.1

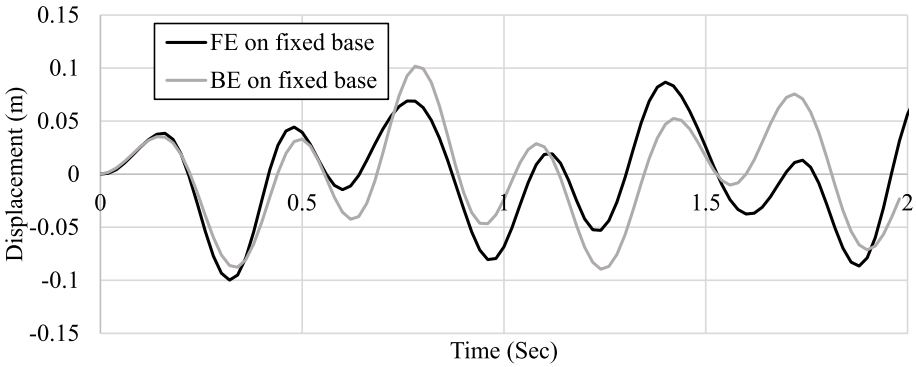

Fig. 10 Top lateral displacement on fixed base under harmonic cosine load in example 7.1

Five stories building on raft foundation

The five stories building in section (recall Fig. 3a) is reconsidered to be analyzed including SSI where columns are 0.5×0.5 m. The sub-structure properties are considered with Young's modulus of 100,000 kN/m^2 and Poisson's ratio equals to 0.3. The dynamic analysis is carried out using time step = 0.02 Sec.

To demonstrate the efficiency of the proposed technique, the building is analyzed under the following three different load cases:

1- Case 1: Linear acceleration with maximum value of 0.5 m/sec^2 at 2 s.
2- Case 2: Harmonic cosine acceleration with an amplitude of 10 m/sec^2 and frequency 20 rad/sec.
3- Case 3: Earthquake acceleration record presented in Fig. 8.

In this paper, FEM models are presented to validate the results of the proposed analysis. In this example, two FEM models with different meshes are carried out. In the first mesh, columns are modeled as solid elements ($0.25 \times 0.25 \times 0.50$ m). Slab mesh is considered 0.5×0.5 m with transient elements around columns. The soil underneath the raft is modeled as solid elements $0.5 \times 0.5 \times 0.5$ m and $2.0 \times 2.0 \times 1.0$ m outside the raft using transition elements. In the second mesh, columns are modeled as solid elements ($0.25 \times 0.25 \times 0.50$ m). Slab mesh is considered 0.25×0.25 m. The soil underneath the raft is modeled as solid element $0.25 \times 0.25 \times 0.5$ m and

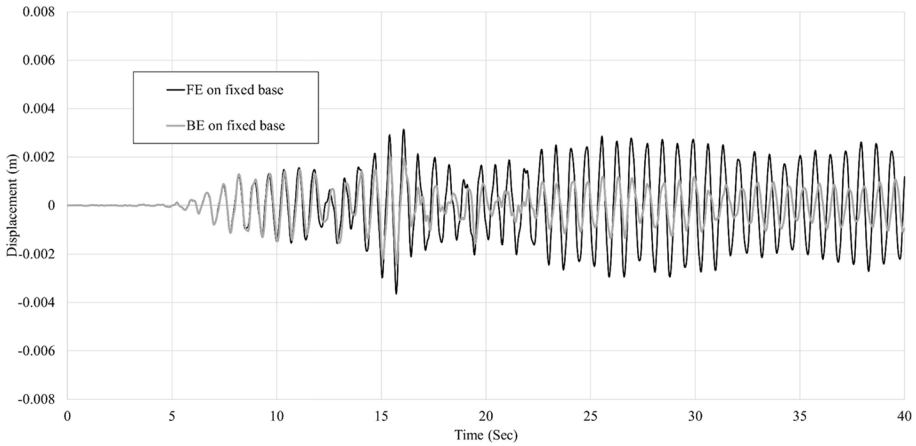

Fig. 11 Top lateral displacement on fixed base under earthquake load in example 7.1

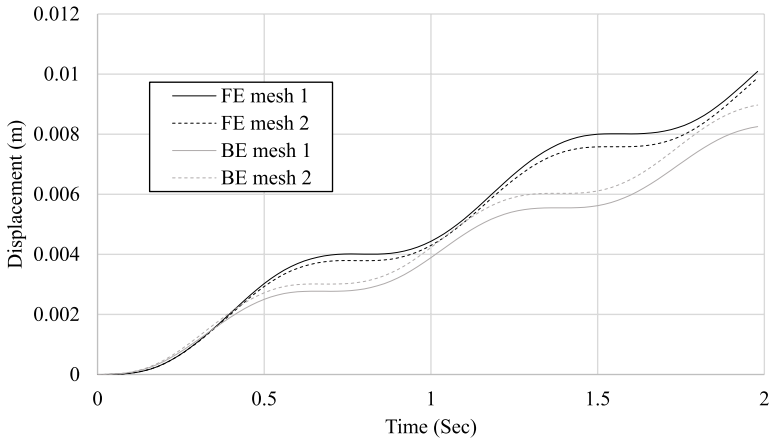

Fig. 12 Top lateral displacement including SSI under linear load in example 7.1

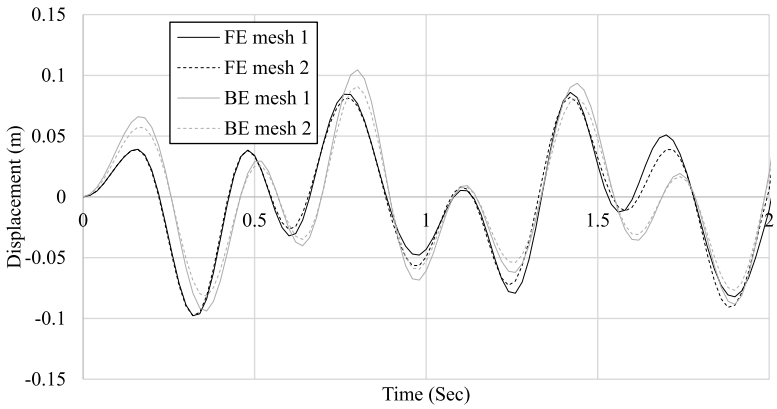

Fig. 13 Top lateral displacement including SSI under cosine load in example 7.1

$1.0 \times 1.0 \times 1.0$ m outside the raft using transition elements. Concerning the soil volume considered, different volumes are analyzed to determine an appropriate soil volume as presented in Appendix.

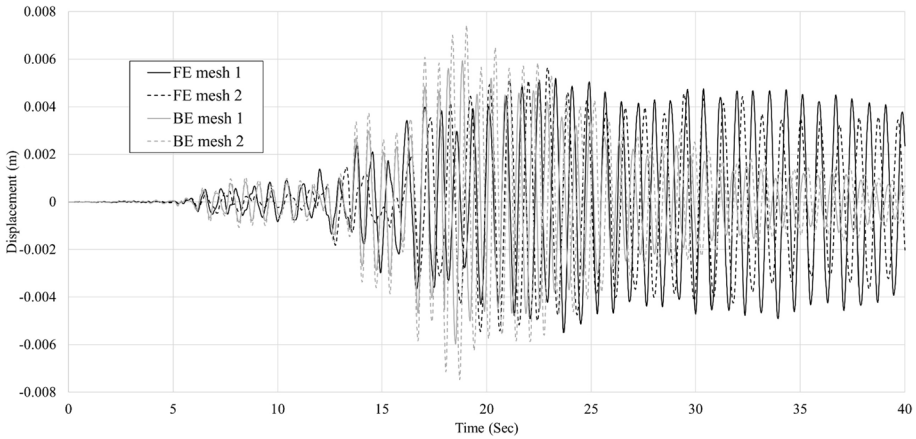

Fig. 14 Top lateral displacement including SSI under earthquake loading example 7.1

Table 1 Comparison of time and storage in example 7.1

	FEM		BEM	
	Mesh 1	**Mesh 2**	**Mesh 1**	**Mesh 2**
No. of DOFs	90,000	448,000	9,546	28,890
Analysis Time (Mins)	32	188	17	90
Memory (Gigabyte)	22.2	130	8	47

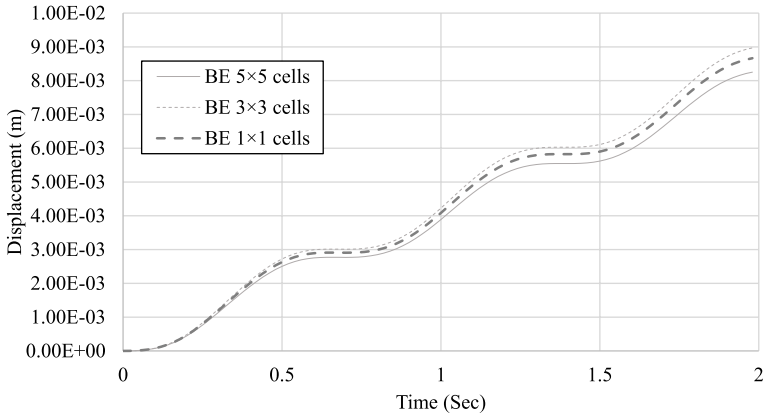

Fig. 15 Top lateral displacement considering different number of coupling cells in example 7.1

Two boundary element meshes are presented. Columns are modeled as four area contact cells. The sub-structure is modeled as 3D boundary element with 5×5 m and 3×3 m for the first and second mesh respectively.

The top lateral displacement of the structure analyzed on fixed base is presented in (Figs. 9, 10 and 11) due to linear, harmonic, earthquake dynamic loads respectively. It has to be noted that, the response gives some difference between FEM and BEM due to column modeling issue that is discussed in Sect. 5.

The top lateral displacement of the building including SSI effect is presented in (Figs. 12, 13 and 14) under the same three different load cases. Ten and five coupling

iterations for the two different models are performed respectively until the convergence criteria (5%) is achieved. The SSI effects increase the displacement by around 15%. The proposed analysis gives results in good agreement with the results obtained from FE analysis and that difference appears due to the area model issue (recall Sect. 5).

Concerning the practicality of the proposed technique, three computational parameters are compared. The number of degrees of freedoms (DOFs), analysis time, and required storage for each model are presented in Table 1. The proposed technique analysis time is almost 50% of the analysis time using FEM models. The required storage is around 36% of the storage required using FEM model which is not convenient in practical examples. In addition, the FE solid elements modeling for vertical elements is extremely difficult in practical examples.

Effect of coupling area cells for the practical building

In this example, the previous example in Fig. 3 is reconsidered to demonstrate the number of coupling area cells effect. Three different meshes of coupling cells are considered. The three meshes are 5×5 m, 3×3 m, 1×1 m coupling cells. The top lateral displacement is demonstrated in Fig. 15. The top lateral displacement changed slightly and localized with different coupling cells. The required number of iterations for the convergence limit (5%) is 10, 5, 3 iterations for the three coupling cells meshes respectively. Therefore, the number of coupling cells affects the number of iterations required for convergence.

Conclusions

Time domain analysis of buildings considering soil-structure interaction is presented. Sub-structuring technique was proposed for two separate structures. An iterative coupling scheme was proposed to allow using different software and to decrease the computational efforts. The super-structure was modeled using BEM to consider the real area model to calculate the relevant stiffness and mass matrices. The sub-structure was modeled using DRM as closed domain without domain discretization. It was demonstrated that the numerical model of the vertical element of the super-structure is strongly affecting the lateral response. The FEM frame element model gives inaccurate response compared to solid elements with an error about (26 – 225) %. The BEM one area cell gives inaccurate response compared to four area cells with an error about (11 – 38) %.

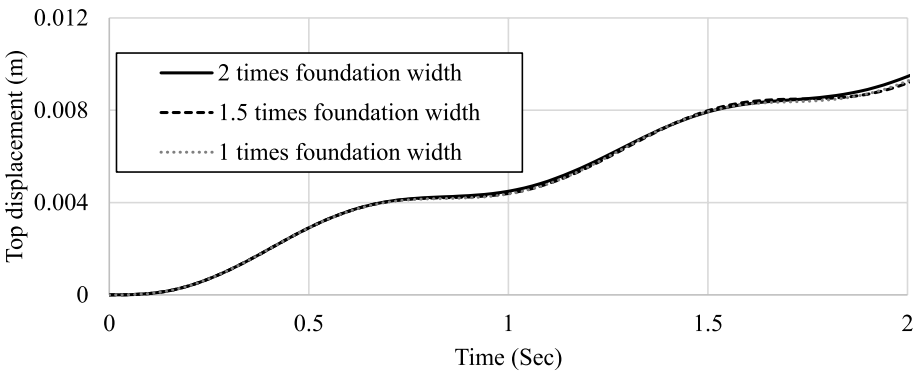

Fig. 16 Top lateral displacement under different soil volumes

The number of coupling cells in the proposed analysis effect is not significant. Practical example under different dynamic excitations is presented. The effect of SSI increases the lateral response by about 15% computed to those of the fixed base analysis. The proposed practical dynamic analysis reduces the time of the analysis to about 50% of that of FEM analysis time and consumes storage around 36% of that used in FEM models.

Appendix

In this appendix, the effect of the soil volume considered in the analysis is presented. The soil block under the building considered in example 6.1 is extended after the raft foundations to 1, 1.5, 2 times of the foundation width. The lateral top displacement is presented in Fig. 16. The results are in a good agreement. The effect of soil block width after 1.5 times the foundation width is neglected. Therefore, in the presented examples, the soil block is extended 1.5 times the foundation width.

Abbreviations

DOFs	Degree of freedoms
$[K_{super}]$	Super-structure stiffness matrix
$[M_{super}]$	Super-structure mass matrix
N_{FL}	The number of floors
N_{cells}	The number of coupling area cells
N_1	The total super-structure considered DOFs ($3N_{FL}+N_{cells}$)
$\left[K_{super22}^{fixed}\right]$	The super-structure stiffness matrix condensed at the vertical DOFs of the coupling area cells
$\left[K_{springs}\right]^{t+\Delta t}$	The coupling area cells vertical springs stiffness matrix at current time step ($t+\Delta t$)
Δt	The chosen time step in transient analysis
$P^{t+\Delta t}$	Equivalent dynamic loading on super-structure floors
$R_{t+\Delta t}$	The super-structure reactions
λ, μ	Lamés constants
$[H_{sub}]$	Sub-structure traction fundamental solution
$[G_{sub}]$	Sub-structure displacement fundamental solution
$\{u_{sub}\}$	Sub-structure displacement field
$\{t_{sub}\}$	Sub-structure traction field
$[\widehat{u}]$	Particular solution of displacement
$\left[\widehat{t}\right]$	Particular solution of traction
M	The number of boundary nodes
K	The number of DRM collocation nodes
[F]	The radial basis function matrix
$[M_{sub}]$	Sub-structure equivalent mass matrix
ρ	Material density
$[A_{sub}]$	Rearranged $\left[\frac{2}{\Delta t^2}[M_{SUB}]+[H_{sub}]\right]$ matrix
$[G_{1sub}]$	Rearranged $[G_{sub}]$ matrix
$\{x_{sub}^{t+\Delta t}\}$	The unknown field vectors at the current time step ($t+\Delta t$)
$\{b_{sub}^{t+\Delta t}\}$	The known field vectors at the current time step ($t+\Delta t$)
$\left\{u_{super}^{t+\Delta t}\right\}$	The super-structure displacement field at the current time step ($t+\Delta t$)

Acknowledgements
Not applicable.

Authors' contributions
All authors have read and approved the manuscript. OES Programming and implementation, carried out the models, writing the paper. AFF Mathematical formulation, review the programming, models, and the manuscript. YFR Review the mathematical formulation, read and approved the final manuscript.

Funding
There is no fund for this manuscript.

Availability of data and materials
The data sets used and analyzed during the current study are available from the corresponding author on reasonable request.

Declarations

Competing interests
The authors declare that they have no competing interests.

Received: 12 April 2023 Accepted: 10 June 2023
Published online: 23 June 2023

References

1. Fathizadeh S, Vosoughi A, Banan R (2021) Considering soil–structure interaction effects on performance-based design optimization of moment-resisting steel frames by an engineered cluster-based genetic algorithm. Eng Opt 23:440–460
2. Jalali HH, Farzam MF, Gavgani SAM, Bekdas G (2023) Semi-active control of buildings using different control algorithms considering SSI. J build Eng 67:1–18
3. Dominguez J (1993) Boundary Element in Dynamics. Computational mechanics publications, Southampton Boston
4. Zhang W, Seylabi E, Taciroglu E (2019) An ABAQUS toolbox for soil-structure interaction analysis. Comp and Geot 114:103–143
5. Yahyai M, Mirtaheri M, Mahoutian M, Daryan A, Assareh M (2008) Soil structure interaction between two adjacent buildings under earthquake load. Amer j of engand App Sc 2:121–125
6. Requena-Garcia-Cruz MV, Bento R, Durand-Neyra A-E (2022) Analysis of the soil structure-interaction effects on the seismic vulnerability of mid-rise RC buildings in Lisbon. Structures 38:599–617
7. Ibrahim Y, Nabil M (2021) Finite element analysis of multistory structures subjected to train-induced vibrations considering soil-structure interaction. C St in Const Mat 15:1–18
8. Abdelwahab M, Rashed YF, A., Mukhtar. (2014) Dynamic boundary element analysis of multistory buildings. J of Eng and App Sc 61:249–268
9. Abdelwahab M, Rashed YF, Mukhtar A (2015) Time history boundary element analysis of multistory buildings. J of Eng and App Sc 62:165–185
10. Chopra A (1981) Dynamics of structures – Theory and applications to earthquake engineering. Prentice hall, New Jersey
11. Wolf JB (1998) Simple physical models for foundation dynamics. Dev in Geot Eng 83:1–70
12. Lysmer J, Kuhlemeyer L (1969) Finite dynamic model for infinite media. J of Eng Mech Div 1:129–131
13. Smith D (1974) A nonreflecting plane boundary for wave propagation problems. J of Comp Phy 15:492–503
14. Bakhtaoui Y, Chelghoum A (2020) Solution for soil–structure interaction with direct infinite element in time domain. Ind Geot J 4:655–663
15. Su J, Wang Y (2013) Equivalent dynamic infinite element for soil-structure interaction. Fin Elem in Anal and Des 63:1–7
16. Robertson LA (1966) Forced vertical vibration of a rigid circular disc on a semi-infinite elastic solid. Proc Camb Phil Soc 62:547–553
17. Luco JE, Westmann RA (1972) Dynamic response of a rigid footing bonded to an elastic half space. J of App Mech 39:527–534
18. Karabalis D, Beskos D (1984) Dynamic response of 3-D rigid surface foundations by the time domain boundary element method. Earth Eng and Struc Dyn 12:73–93
19. Karabalis D, Beskos D (1986) Dynamic response of 3-D embedded foundations by the boundary element method. Comp Meth in App Mech and Eng 56:91–119
20. Karabalis D (1991) A simplified 3-D time domain BEM for dynamic soil – structure interaction problem. Eng Anal with Boun Elem 8:139–145
21. Karabali D, Huang C (1994) 3-D foundation-soil-foundation interaction. Tran on Mod and Sim 8:197–209
22. Spyrakos C, Beskos D (1986) Dynamic response of rigid strip-foundations by a time-domain boundary element method. Int j for Num Meth in Eng 23:1547–1565
23. Rashed YF (2002) Transient dynamic boundary element analysis using Gaussian-based mass matrix. Eng Anl Bound Elem 26:265–279
24. Rashed YF (2008) Free vibration of structures with trignometric SIN(R) function in the dual reciprocity boundary element analysis. Adv Struc Eng 11:397–409
25. Samaan MF, Rashed YF, Ahmed MA (2007) The dual reciprocity method applied to free vibrations of 2D structures using compact supported radial basis functions. Comp Mech 41:85–105
26. Samaan MF, Rashed YF (2007) BEM for transient 2D elastodynamics using multiquadric functions. Int J Sol Mech 44:8517–8531
27. Partridge P, Brebbia C, Wrobel L (1991) The dual reciprocity boundary element method. Springer, Dordrecht
28. J. Ananias's, D. Polyzos, D. Besko, (1998) Three-dimensional structural vibration analysis by the dual reciprocity BEM. Comp Mech 21:387–381
29. Kog M, Gaul L (2000) A 3-D boundary element method for dynamic analysis of anisotropic elastic solids. Comp Mod in Eng and Sc 1:27–43

30. Galvis A, Prada D, Moura L, Zavaglia C, Foster J, Sollero P, Wrobel L (2021) BESLE: boundary element software for 3D linear elasticity. Comp Phy Com 265:1–39
31. Ibrahim AA, Farid AF, Rashed YF, El-Attar M (2022) New three-dimensional time-stepping transient fundamental solutions with applications. Eng Anal Bound Elem 144:352–365
32. Farid AF, Rashed YF (2022) Time-differencing fundamental solutions for plane elastodynamics. ASCE-J Eng Mech. 148(8):04022035
33. C. A. Berrebia (1987) Topics in boundary element research- volume 4 applications in geomechanics. Springer-Verlag Berlin Heidelberg
34. Hatzigeorgiou G, Beskos D (2001) Transient dynamic response of 3-D elastoplastic structures by the D/BEM. Tran on Mod and Sim 28:129–137
35. Lei W, Liu C, Li H, Qin X, Chen R (2018) Iterative coupling of precise integration FEM and TD-BEM for elastodynamic analysis. Struc Eng and Mech 67:317–326
36. Elmeliegy AM, Rashed YF (2019) Efficient preconditioned soil–foundation–structure interaction approach to compute tall-building time periods. Pract Period Struct Des Const 24:04019007
37. Torky AA, Rashed YF (2020) High-performance practical stiffness analysis of high-rise buildings using superfloor elements. J Comp Des Eng 7:211–227
38. Hassan AMM, Torky AA, Rashed YF (2019) Geometrically accurate structural analysis models in BIM-centered software. Autom Const 104:299–321
39. Bathe KJ (1982) Finite element procedures in engineering analysis. Prentice-Hall
40. Gaul L, Kögl M, Wagner M (2003) Boundary Element Methods for Engineers and Scientists. Springer, Berlin
41. Wagdy M, Rashed YF (2014) Boundary element analysis of multi-thickness shear-deformable slabs without subregions. Eng Anal Bound Elem 43:86–94

Publisher's Note